



**Queensland University of Technology**  
Brisbane Australia

This is the author's version of a work that was submitted/accepted for publication in the following source:

Cheung, Joe, Morawska, Lidia, & Ristovski, Zoran (2011) Observation of new particle formation in subtropical urban environment. *Atmospheric Chemistry and Physics (ACP) & Discussions (ACPD)*, 11, pp. 3823-3833.

This file was downloaded from: <http://eprints.qut.edu.au/53519/>

© Copyright 2012 The author.

**Notice:** *Changes introduced as a result of publishing processes such as copy-editing and formatting may not be reflected in this document. For a definitive version of this work, please refer to the published source:*

<http://dx.doi.org/10.5194/acp-11-3823-2011>

# 1 **Observation of new particle formation in subtropical urban environment**

2  
3 H.C. CHEUNG, L. MORAWSKA\* and Z.D. RISTOVSKI

4 International Laboratory of Air Quality and Health, Queensland University of Technology,  
5 GPO Box 2434, Brisbane QLD 4001, Australia

6  
7 \*Corresponding Author:

8 Telephone - 61 7 3138 2616

9 Fax - 61 7 3138 9079

10 E-mail - [l.morawska@qut.edu.au](mailto:l.morawska@qut.edu.au)

## 11 12 **Abstract**

13 The aim of this study was to characterise the new particle formation events in a subtropical  
14 urban environment in the southern hemisphere. The study measured the number  
15 concentration of particles and its size distribution in Brisbane, Australia during 2009. The  
16 variation of particle number concentration and nucleation burst events were characterised as  
17 well as the particle growth rate which was first reported in urban environment of Australia.  
18 The annual average  $N_{\text{UFP}}$ ,  $N_{\text{Aitken}}$  and  $N_{\text{Nuc}}$  were  $9.3 \times 10^3$ ,  $3.7 \times 10^3$  and  $5.6 \times 10^3 \text{ cm}^{-3}$ ,  
19 respectively. Weak seasonal variation in number concentration was observed. Local traffic  
20 exhaust emissions were a major contributor of the pollution ( $N_{\text{UFP}}$ ) observed in morning  
21 which was dominated by the Aitken mode particles, while particles formed by secondary  
22 formation processes contributed to the particle number concentration during afternoon.  
23 Overall, 65 nucleation burst events were identified during the study period. Nucleation burst  
24 events were classified into two groups, with and without particles growth after the burst of  
25 nucleation mode particles observed. The average particle growth rate of the nucleation events  
26 was  $4.6 \text{ nm hr}^{-1}$  (ranged from  $1.79 - 7.78 \text{ nm hr}^{-1}$ ). Case studies of the nucleation burst events  
27 were characterised including i) the nucleation burst with particle growth which is associated  
28 with the particle precursor emitted from local traffic exhaust emission, ii) the nucleation burst  
29 without particle growth which is due to the transport of industrial emissions from the coast to  
30 Brisbane city or other possible sources with unfavourable conditions which suppressed  
31 particle growth and iii) interplay between the above two cases which demonstrated the impact  
32 of the vehicle and industrial emissions on the variation of particle number concentration and  
33 its size distribution during the same day.

1

## 2 1. Introduction

3 Understanding the formation process of atmospheric particles is vital because of the  
4 significant impact of particulate matter on human health and climate change (Charlson et al.,  
5 1992, Donaldson et al., 1998). Atmospheric particles can be formed by nucleation process via  
6 a number of different mechanisms (e.g. Kulmala 2003; Kulmala et al., 2004), such as binary  
7 nucleation (involving  $\text{H}_2\text{SO}_4$  and water vapour), ternary nucleation (involving  $\text{NH}_3$ ,  $\text{H}_2\text{SO}_4$   
8 and water vapour) and ion-induced nucleation for charged particles, depending on the  
9 environmental conditions. To date, numerous studies have been conducted in different  
10 locations, in order to investigate particle formation processes in different environmental  
11 settings, including the free troposphere (e.g. Weber et al., 2001), boreal forests (e.g.  
12 Vehkamäki et al., 2004) and coastal areas (e.g. O'Dowd et al., 1999; Lee et al., 2008).  
13 However, most of these studies focused on particle formation in rural settings and in colder  
14 climates, with very few studies conducted in urban environments, especially in the southern  
15 hemisphere (Kulmala et al., 2004). A limited number of studies were conducted in  
16 continental (e.g. Woo et al., 2001; Moore et al., 2007; Wu et al., 2008) and coastal (Pey et al.,  
17 2008; Rodríguez et al., 2008; Fernández-Camacho et al., 2010; Pérez et al., 2010) urban areas.  
18 These studies examined the variation of particle number concentration in urban environments.  
19 The major influence on particle number concentration was vehicle exhaust emissions during  
20 the traffic peak hours (e.g. Pey et al., 2008; Pérez et al., 2010) and new particle formation by  
21 photochemical reactions (e.g. Pey et al., 2009), as well as the influence of power plant and  
22 industrial emissions from an area upwind from the urban site (Gao et al., 2009). The few  
23 examples include studies on particle formation associated with natural emissions from a  
24 Eucalypt forest in South-East Australia (Ristovski et al., 2010; Suni et al., 2008), which  
25 concluded that natural emissions were in fact a source of particle formation. In addition, new  
26 particle formation was observed in the coastal area of Eastern Australia (Johnson et al., 2005;  
27 Modini et al., 2009), the result of which showed that new particles were formed by the  
28 condensation of sulphate and/or organic vapours onto sulphate clusters to form an observable  
29 particle. Guo et al. (2008) conducted a short-term intensive study on particle formation in the  
30 rural environment of Eastern Australia, in which particle formation was suggested to be  
31 influenced by the photochemical processes of the urban air plume. The findings of Guo et al.  
32 (2008) provided an insight to the impact of urban pollution on nucleation processes. For the  
33 urban environment, Mejía et al. (2009) characterised the favourable atmospheric conditions  
34 for nucleation burst events in a coastal urban area in Brisbane, which is the only nucleation  
35 study conducted in an urban area in the southern hemisphere to date. The study showed that  
36 the nucleation events mostly occurred during the summer and it also suggested cleaner air  
37 masses of a local origin mixing with traffic exhaust emission after the events. However, Mejía  
38 a et al. (2009) did not investigate the nucleation growth process after the nucleation burst  
39 events, and thus particle formation parameters, such as particle growth rate, are not available  
40 for the urban environment in southern hemisphere. The particle growth rate is an important  
41 factor for the calculation of climate forcing.

42 To further investigate the characteristics of the particle formation processes in a subtropical  
43 urban environment, we conducted a one year-long measurement of the size distribution of  
44 particles in the size range 4 – 110 nm, at an urban area of Brisbane, Australia. The aim of this  
45 study was to characterise the temporal variation of particle number concentration, and to

1 explain the controlling factors that influenced new particle formation processes in the  
2 subtropical urban environment.

3

## 4 2. Methodology

### 5 2.1 The topography and meteorology of Brisbane region

6 Brisbane is the capital city of the state of Queensland, Australia, located at 27°30'S and 153°E.  
7 Brisbane city is surrounded by mountains from south to north, and faces the Pacific Ocean to the East.  
8 It is the fastest growing urban region in Australia (2 million inhabitants). The major pollution  
9 sources affecting the CBD region are traffic exhaust emissions generated in the inner city,  
10 and aircrafts, ships and industrial emissions transported from the lower reaches of Brisbane  
11 River, approximately 15-18 kms NE of the CBD. The Brisbane River meanders through the  
12 Brisbane region.

13 Morawska et al. (1998) provided a description of the wind patterns in the Brisbane region,  
14 which are mostly governed by synoptic flows from the SE. A NE sea breeze is also a daily  
15 feature throughout the year. In addition, an overnight SW drainage flow from the mountain  
16 range to the West carries air parcels from the plateau region and the Western coastal plain  
17 towards the city. On the rare occasion when gradient winds are blowing from the NW, the  
18 combination of the light synoptic NW flow and the overnight SW drainage flow can  
19 sufficiently delay the onset of the sea breeze to cause recirculation of the city emissions,  
20 leading to photochemical smog events.

### 21 2.2 The QUT study site

22 The measurements were conducted at the International Laboratory of Air Quality and Health  
23 (ILAQH), Queensland University of Technology (QUT), which is within the CBD of  
24 Brisbane (**Figure 1**). The monitoring site was about 10 m above ground level on the top floor  
25 of a QUT campus building, located to the SE of the city centre, with a major highway (the  
26 Pacific Motorway) situated along the SW side of the campus. Therefore, the pollution  
27 associated NE winds could be attributed to industrial emissions (from the airport, oil refinery  
28 and Port of Brisbane), while the pollution associated with S to NW winds could be attributed  
29 to local traffic exhaust emissions.

### 30 2.3 Measurement techniques

31 The size distribution of ultrafine particles (UFPs) was measured at the QUT monitoring site  
32 from 1<sup>st</sup> January to 31<sup>st</sup> December 2009. Particle size distribution in the range 4 - 110 nm was  
33 measured by a Scanning Mobility Particle Sizer (SMPS) system, which consisted of two parts,  
34 an Electrostatic Classifier (EC) (TSI 3080) and a Condensation Particle Counter (CPC) (TSI  
35 3781). The EC was equipped with a nano-differential mobility analyser, which can separate  
36 the poly-disperse particles into selected mono-disperse particles according to their particle  
37 mobility. The number concentration of the mono-disperse particles was then counted by the  
38 CPC. Each ambient sample was drawn into the SMPS system from outside the building  
39 through a 0.635 cm (inner diameter) conductive tube and a sampling duration of 5 mins was  
40 adopted for each particle size distribution sample. Multiple charge correction was applied to  
41 the particle size distribution measurements by using an internal algorithm from the Aerosol  
42 Instrument Manager Software.

1 In this study, the size distribution data was classified into three groups, i) UFPs, including  
2 particles ranging from 4 - 110 nm ( $N_{\text{UFP}}$ ); ii) Aitken mode with particles ( $N_{\text{Aitken}}$ ), which  
3 ranged from 30 - 110 nm; and iii) nucleation mode particles, which were  $< 30$  nm ( $N_{\text{nuc}}$ ). In  
4 addition to the above particle measurements, meteorological parameters, including wind  
5 speed and direction, temperature and relative humidity (RH) were monitored at Kangaroo  
6 Point (1 km East of QUT) by the Queensland Bureau of Meteorology. The QUT and  
7 Kangaroo Point sites were not blocked by high rise buildings and therefore the use of wind  
8 data measured at Kangaroo Point was representative of the synoptic wind direction of the  
9 study region. It should be noted that global solar radiation was measured at the Queensland  
10 Environmental Protection Agency site (Rocklea), about 10 km south of QUT.

## 11 2.4 Data processing and analysis

12 In this study, the raw particle size distribution and meteorological data were synchronised  
13 into 10 min averaged data for data analysis and figure plotting. According to Mejía et al.  
14 (2007) the lower limit of the particle size distribution dataset was set to  $1 \text{ cm}^{-3}$ . The upper  
15 limit was set to  $5 \times 10^5 \text{ cm}^{-3}$ . Some data were removed from the database based on several  
16 criteria such as i) zero value for particle concentration; ii) particle concentration higher than  $5$   
17  $\times 10^5 \text{ cm}^{-3}$  and iii) data collected during instrument malfunction. During the one year  
18 measurement campaign, 28 % of the data was removed based on the above data reduction  
19 procedures and due to instrument maintenance. Correlations between the parameters were  
20 tested using the Pearson-product moment correlations test with a 95% confidence level ( $p <$   
21  $0.05$ ). The linearity of the tested parameters was indicated by Pearson's coefficient,  $r$ , with a  
22 perfect linear correlation between two parameters indicated by an  $r$  value close to 1.

23

## 24 3. Results and Discussion

### 25 3.1 Overall results

26 The overall average concentration of ultrafine particles ( $N_{\text{UFP}}$ ), Aitken mode ( $N_{\text{Aitken}}$ ) and  
27 nucleation mode ( $N_{\text{nuc}}$ ) measured in this study were  $9.3 \times 10^3 (\pm 15.3 \times 10^3)$ ,  $3.7 \times 10^3 (\pm 5.1 \times$   
28  $10^3)$  and  $5.6 \times 10^3 \text{ cm}^{-3} (\pm 12.6 \times 10^3)$ , respectively. The values obtained in this study are  
29 similar to those observed in similar environments in Northern Europe (Hussein et al., 2004).  
30 The few studies conducted in Southern European countries showed much higher  
31 concentrations than those which were reported in this study (Pey et al., 2008, Rodríguez et al.,  
32 2008; Fernández-Camacho et al., 2010). Similar values of  $N_{\text{Aitken}}$  and  $N_{\text{nuc}}$  were obtained in  
33 the urban areas of Helsinki, Finland, which were  $4.0 \times 10^3 - 6.5 \times 10^3 \text{ cm}^{-3}$  and  $5.5 \times 10^3 -$   
34  $7.0 \times 10^3 \text{ cm}^{-3}$ , respectively (Hussein et al., 2004). The  $N_{\text{UFP}}$  measured in Brisbane was  
35 relatively lower than that in other coastal urban areas, including the Yangtze River Delta,  
36 China (Gao et al., 2009), Barcelona (Pey et al., 2008) and Huelva and Santa Cruz de Tenerife,  
37 Spain (Rodríguez et al., 2008; Fernández-Camacho et al., 2010), which were  $28.5 \times 10^3$ ,  $14.2$   
38  $\times 10^3$  and  $22.0 - 26.3 \times 10^3 \text{ cm}^{-3}$ , respectively.

39 The results of this study were also compared to those of a previous study conducted in the  
40 Brisbane urban region from 1995 to 2000 (Mejía et al., 2007). The  $N_{\text{UFP}}$  and  $N_{\text{nuc}}$  measured in  
41 this study were about 8% and 60% higher than those measured by Mejía et al. (2007), being  
42  $8.6 \times 10^3 \text{ cm}^{-3}$  (for particles in the size range 15 - 100 nm) and  $3.5 \times 10^3 \text{ cm}^{-3}$  (for particles in  
43 the size range 15 - 30 nm), respectively. In relation to  $N_{\text{nuc}}$ , it should be noted that the

1 nucleation mode particle concentration in this study covered particles in the size range 4 - 30  
2 nm, and therefore, it is expected to be higher than the earlier result reported by Mejía et al.  
3 (2007).

4 The seasonal variation of particle number concentrations is depicted in **Figure 2**. The  
5 Pearson's coefficients,  $r$ , between particle number concentration of different modes and  
6 temperature were calculated which ranged from 0.00 - 0.03, which indicates that there was no  
7 statistical seasonal variation in particle concentrations. This result is similar to that presented  
8 by Mejía et al. (2007) for the same study region, however larger variations in particle number  
9 concentrations were observed in each mode during the summer season, as reflected by the  
10 large interquartile range (see **Figure 2**).

11 **Figure 3** shows the diurnal variation of particle number concentration for different modes  
12 with the diurnal variations of temperature and relative humidity also plotted. Two peaks were  
13 observed for UFP during the day, the first of which occurred from around 6 am to 8 am,  
14 possibly due to traffic exhaust emissions during the morning peak hours (from around 6 am  
15 to 8 am) in Brisbane urban region (Mejía et al., 2007). The second peak, which is much more  
16 important, was observed from around 12 noon to 3 pm, and this may be due to the formation  
17 of new particles. During the period of UFP morning peak, it was suggested that the Aitken  
18 mode particles contributed by the direct diesel and petrol engine emissions, which produce  
19 particles in the size range of about 20 – 130 nm and 20 – 60 nm, respectively (Morawska et  
20 al., 2008). Also the nucleation mode particles could be formed during the dilution and  
21 cooling of engine exhausted sulphuric and organic vapours by condensation onto sulphur  
22 clusters (Meyer and Ristovski 2007). During the period of the second UFP peak, a nucleation  
23 mode peak was also observed associated with highest level of solar radiation, which implies  
24 that new particles were produced during the early afternoon by photochemical reactions.

## 25 3.2 Relationship between particle number concentrations and meteorological parameters

### 26 3.2.1 Temperature, relative humidity and solar radiation

27 From **Figure 3** it can be seen that temperature and relative humidity display an anti-  
28 correlation, whereby increases in temperature were associated with decreases in relative  
29 humidity. The influences of temperature on particle number concentration were not  
30 confirmed in previous studies. Some studies found that high particle concentration was  
31 related to relatively high temperatures (e.g. Kim et al., 2002), whilst others found that they  
32 were associated with relatively low temperatures (e.g. Olivares et al., 2007). In this study, a  
33 weak correlation between particle number concentrations and temperature was observed ( $r =$   
34  $0.36 - 0.53$ ;  $p < 0.01$ ), however higher variations in  $N_{\text{UFP}}$ ,  $N_{\text{Aitken}}$  and  $N_{\text{nuc}}$  were observed  
35 during warmer and lower humidity conditions (**Figures 4 and 5**). The highest number  
36 concentrations of all particle sizes were associated with temperature around 32°C. The peaks  
37 of  $N_{\text{Aitken}}$  and  $N_{\text{nuc}}$  observed in the early afternoon (under high temperature conditions)  
38 suggested that the contribution by new particle formation processes was the greatest,  
39 followed by particle growth to larger particles. In addition, another peak of  $N_{\text{Aitken}}$  was  
40 observed with temperature around 10°C (see **Figure 4**). Also higher  $N_{\text{Aitken}}$  concentrations  
41 were observed under humid conditions (see **Figure 5**). This result may be due to enhanced  
42 coagulation and condensation effects under high humidity conditions.

43 In some cases, temperature data can not directly reflect the strength of photochemical  
44 activities which occurred on warm cloudy days. In addition, condensation vapour  $\text{H}_2\text{SO}_4$

1 production was related to the solar radiation (Ristovski et al., 2010). Therefore, solar  
2 radiation was used to indicate the reactivity of photochemical reactions. The particle number  
3 concentration did not show a clear relationship with the ambient temperature. In contrast, a  
4 positive relationship between particle number concentration and solar radiation data was  
5 observed ( $r = 0.92-0.98$ ;  $p < 0.01$ ). This result showed that the  $N_{\text{nuc}}$  was related to the  
6 photochemical reactions.

### 7 3.2.2 Wind direction and speed

8 **Figure 6** shows the particle number concentration for different particle sizes under different  
9 wind directions. For UFP, a sharp peak was associated with ENE wind directions, and a  
10 lower broad peak was associated with SSE to WNW wind directions. An interesting result  
11 was also obtained when dividing the data into Aitken and nucleation modes. The sharp peak  
12 was observed in both of these two modes, however the broad peak was only observed in the  
13 Aitken mode. From **Figure 1**, it can be seen that the Brisbane Airport, oil refinery and Port of  
14 Brisbane were all located to the NE of the monitoring site, whilst the CBD and Pacific  
15 Motorway were located to the NW and SW of the monitoring site. Therefore, it is likely that  
16 the nucleation mode particles were contributed by the industrial sources located to the NE,  
17 while the Aitken mode particles were emitted from both industrial and vehicle emission  
18 sources, as well as the coagulation/condensation of smaller particles under humid conditions  
19 (see section 3.2.1), which will contribute to the accumulation mode. In addition, air masses  
20 blowing from the marine boundary (NE to SE directions) were relatively clean. However, the  
21 inland air mass from the NE direction was contaminated by industrial emissions. This  
22 interpretation can be supported by higher  $N_{\text{UFP}}$  in north-easterly air masses and lower  $N_{\text{UFP}}$  in  
23 easterly or south-easterly air masses (clean maritime air masses, which are thought to be  
24 much less loaded in gaseous precursors). To better illustrate the directional dependence of the  
25  $N_{\text{UFP}}$ ,  $N_{\text{Aitken}}$  and  $N_{\text{nuc}}$  a wind rose plot of particle number concentration superimposed over  
26 the location map is shown in the supplementary materials section (**Figure S1**).

27 In general, a negative correlation was observed between UFP concentration and wind speed,  
28 indicated by a Pearson coefficient of  $r = -0.97$  ( $p < 0.01$ ). Higher particle number  
29 concentration was associated with lower wind speeds (see **Figure 7**), which can be explained  
30 by the stronger dispersion associated with high wind speeds (Hussein et al., 2006). Similar  
31 results were also observed for Aitken and nucleation mode particles. In addition, a larger  
32 variation of  $N_{\text{nuc}}$  was associated with the moderate wind speed ( $\sim 4 \text{ ms}^{-1}$ ).  $N_{\text{nuc}}$  usually  
33 reached it's daily peak value during early afternoon and the corresponding wind speed was  $\sim$   
34  $4 \text{ ms}^{-1}$  (see **Figure 3**).

## 35 3.3 Particle formation in subtropical urban atmosphere

### 36 3.3.1 Classification of nucleation events

37 The general definition of a nucleation event is a two-phase process involving the burst of  
38 observed nucleation particles and the growth of these particles into accumulation mode by  
39 condensation and/or coagulation (Kulmala et al., 2004). To illustrate the nucleation event, a  
40 “banana” shape should be observed in the contour plot of particle size distribution. The  
41 example of a nucleation event is shown in **Figure 8**. Usually the lowest  $N_{\text{nuc}}$  is observed in  
42 the early morning, and then it begins to increase at around 9 am. The geometric median  
43 diameter (GMD) of the measured particles grows into an Accumulation mode during the day  
44 and the evolvement of the particle size curve is often compared to a banana shape.

1 A number of nucleation events were observed during this study, which were classified into  
2 different groups (Class Ia/b and II) according to the classification scheme developed by Dal  
3 Maso et al. (2005). Class Ia/b events are defined as those events where the particle growth  
4 rate can be determined. A typical Class Ia event demonstrates clear and strong particle  
5 formation events with little or no pre-existing particles obscuring the observation of the  
6 newly formed mode, while a Class Ib event is any other event where the particle growth rate  
7 can be determined. Class II events are defined as events where the banana shape still  
8 observable, but the data fluctuates to such an extent that formation rate calculation is  
9 impractical.

10 In the urban environment, nucleation burst events have been observed with and without  
11 particle growth (Park et al., 2008; Gao et al., 2009). For example, in addition to nucleation  
12 events, we occasionally observed increases in nucleation mode particle concentration during  
13 the daytime, where the particles did not grow into larger particles (indicated by the near  
14 constant GMD value during the event period). We defined this kind of event as a nucleation  
15 burst event, and a total of 65 burst events were identified. A more detailed discussion about  
16 the occurrence of nucleation events, both with and without particle growth, is provided in  
17 Section 3.3.2 and 3.4 below.

### 18 3.3.2 Growth rate during nucleation events

19 During this study, there were several gaps in the dataset due to instrument  
20 malfunction/maintenance. For example, if there were more than 3 hrs of missed data between  
21 8 am to 6 pm (the period during which the nucleation usually occurs), this was not counted as  
22 a valid daily dataset. After the removal of invalid daily datasets, a total of 252 days of data  
23 were counted.

24 **Figure 9** shows the monthly averaged particle growth rate and solar radiation, as well as the  
25 monthly occurrence of nucleation events. This data provided information regarding the  
26 influence of photochemical activity on particle formation in Brisbane. Higher particle growth  
27 rate was found to be associated with higher solar radiation and the results showed a positive  
28 relationship ( $r = 0.76$ ,  $p < 0.05$ ) between the particle growth rate of nucleation events and  
29 solar radiation. Similar findings were obtained in previous studies, which showed that particle  
30 growth rates were associated with the strength of solar radiation (e.g. Kulmala et al., 2004;  
31 Vehkamäki et al., 2004). The number of nucleation events classified as Class Ia, Ib, and II  
32 were 4, 13, and 23, respectively. The nucleation events (Class I and II) occurred throughout  
33 most of the year, except in November, and only one Class II event was observed in December.  
34 Although infrequent nucleation events were observed during November and December, the  
35 nucleation bursts (without particle growth) were found to be closely associated with NE wind  
36 directions. In addition to the seasonal variation of temperature, the dominant wind direction  
37 measured during November and December was different to other months. NE winds  
38 dominated during these warmer months, while the main wind direction was from the SE-SW  
39 during other months. The influence of wind direction on the nucleation events will be  
40 discussed in the case studies below. The mean growth rate for the nucleation events was  
41 calculated by the slope of GMD against time during the period of particle growth under 30  
42 nm. The growth rates of Class I events measured in this study ranged from 1.79 - 7.78 nm hr<sup>-1</sup>  
43 (average 4.6 nm hr<sup>-1</sup>), which are comparable to other urban studies such as those conducted in  
44 Atlanta (2.86 - 22.0 nm hr<sup>-1</sup>) (Woo et al., 2001) and East St. Louis (average 6.7 nm hr<sup>-1</sup>)  
45 (Qian et al., 2007).



1

## 2 3.4 Case studies of nucleation burst events

3 In the above sections, it was shown that nucleation mode particle concentrations were  
4 strongly associated with NE/SW winds. Further analysis of the daily variation of particles and  
5 wind direction showed that nucleation events with particle growth were usually associated  
6 with SW winds, while the nucleation burst events without particle growth were associated  
7 with NW winds. In this section, case studies relating to types of three nucleation events are  
8 discussed, including: i) new particle formation by nucleation processes; ii) a nucleation burst  
9 without particle growth; and iii) the interplay between these two situations.

10

### 11 3.4.1 Case I - Photochemical formation of nucleation particles

12 Case I nucleation events were observed during 28 - 29 April 2009. Significant strong  
13 nucleation bursts were observed consecutively during these two days (peak 10 min and  
14 hourly averaged  $N_{\text{nuc}}$  during the nucleation events were  $47 \times 10^4$  and  $18 \times 10^4 \text{ cm}^{-3}$ ,  
15 respectively). The time series plots of the particle size distribution and meteorological  
16 parameters are illustrated in **Figure 10**.

17 During these two days, the highest temperature was about 30 C and relative humidity was  
18 around 20-40 % at noon. Land and sea breeze wind circulation was observed on both days,  
19 with a moderate ( $\sim 4 \text{ ms}^{-1}$ ) SW wind (from inland) dominating in the morning and a moderate  
20 NE wind (from the coast) dominating in the afternoon. The variation in concentration of  
21 nucleation and Aitken mode particles clearly showed the influence of the nucleation burst on  
22 particle number concentrations. In the early morning (6 - 9 am) of 28 April 2009, an Aitken  
23 mode peak was observed, which could be attributed to traffic exhaust emissions during the  
24 morning peak hours. At around 10 am, a sharp peak of nucleation mode particles was  
25 observed and the GMD reached the lowest value of the day ( $\sim 8 \text{ nm}$ ). The wind direction  
26 changed to NE at around 1 pm, and turned back to the SW again after midnight. In terms of  
27 GMD, the nucleation mode particles were growing into larger particles (GMD increased from  
28 8 to 57 nm) until around midnight ( $\sim 3 \text{ am}$  on 29 April 2009). Another nucleation growth  
29 event was observed the following day, on 29 April 2009, with similar meteorological  
30 conditions to those which were observed on the previous day. However, the concentration of  
31 nucleation particles during the nucleation burst was lower than that observed on the previous  
32 day. This result indicated that the higher number of pre-existing Aitken mode particles in the  
33 atmosphere served to diminish the nucleation processes.

### 34 3.4.2 Case II - nucleation burst without growth into larger particles

35 A Case II nucleation event was observed on 11 November 2009. As shown in **Figure 11**, the  
36 variation in wind direction was similar to that observed during the Case I nucleation events,  
37 whereby land and sea breeze circulation was observed, however, the burst of nucleation  
38 particles did not appear with the SW wind (associated with local traffic exhaust emissions).  
39 Instead, a nucleation burst was observed with the NE wind at  $\sim 10 \text{ am}$ . The GMD dropped  
40 from  $\sim 30 \text{ nm}$  to  $10 \text{ nm}$  and  $N_{\text{nuc}}$  increased from  $\sim 7.0 \times 10^3$  to  $10.0 \times 10^4 \text{ cm}^{-3}$  during the  
41 nucleation burst, while  $N_{\text{Aitken}}$  did not show any significant variation, ranging from  $2 - 5 \times 10^3$   
42  $\text{cm}^{-3}$ . This plume disappeared at around 6 pm and GMD rose to  $\sim 25 \text{ nm}$ . Based on these  
43 findings, it was suggested that the plume was not directly emitted from the local traffic  
44 exhaust emission or ship emission from the Port of Brisbane, since the particles from vehicle  
45 and ship emissions are in the range 20 -130 nm (Morawska et al., 2008) and 60 – 120 nm

1 (Sinha et al., 2003), respectively. However, the emissions of SO<sub>2</sub> and VOCs from the  
2 industrial sources located at the coast could be possible precursors to the formation of new  
3 particles by nucleation process. Another possible source of this plume was aircraft emissions  
4 from the Brisbane Airport, which was located in a NE direction from the study site. Mazaheri  
5 et al. (2009) measured the particle size distribution produced by commercial aircraft at  
6 Brisbane Airport and a very distinct peak of nucleation mode particles was observed at  
7 around 15 nm. This result was comparable to the average GMD measured during the  
8 nucleation burst events in this study, which was 14 nm (ranging from 8 - 32 nm). In addition,  
9 the nucleation burst could be due to the precursors of local emissions which were similar to  
10 that in the nucleation growth event or the re-circulated aged plumes belonging to land and sea  
11 breeze; however the particle growth process could have been suppressed due to unfavourable  
12 conditions, the exact nature of which is not known.

13

#### 14 3.4.3 Case III - Interplay between new particle formation and nucleation burst events

15 A Case III nucleation event was observed on 15 March 2009. During this study, it was found  
16 that particle formation via nucleation processes was associated with SW winds (**Figure 10**)  
17 and the subsequent particle growth (banana shape of particle size distribution) was usually  
18 followed by the presence of a NE wind. In contrast, the nucleation burst events without  
19 particle growth were most commonly related to emission sources from the NE (**Figure 11**).  
20 In some events, a partial banana shape was observed with a SW wind in the morning, but the  
21 observation of particle growth was interrupted by a nucleation burst plume from the airport  
22 region (**Figure 12**).

23 It can be seen that the nucleation process commenced at 9 am and the particles kept growing  
24 into Aitken mode particles until 12 pm (GMD rose from 20 to 35 nm). After 12 pm, the wind  
25 direction changed to a NE wind and an air plume enriched with nucleation mode particles  
26 was observed, which interrupted the observation of a banana shaped progression of the  
27 particle size distribution curve. After the interruption, the GMD dropped suddenly to below  
28 20 nm and several similar cases were also observed during the one year study period at QUT.  
29 Overall, the results showed that the nucleation mode particles originated from a variety of  
30 sources such as traffic exhaust emission in Brisbane CBD and industrial emissions located  
31 NE to Brisbane. Although the observation of a banana shape was interrupted by another air  
32 mass, the particle growth process could continue in other regions.

33

#### 34 3.4.4 Source identification

35 Gaseous data measured at Pinkenba, which is located near the lower reaches of the Brisbane  
36 River (close to the airport, oil refinery and port of Brisbane) and South Brisbane (about 1km  
37 south to QUT) were used to conduct source analysis. These gaseous measurements were  
38 conducted by the Queensland Environmental Protection Agency. Also back-trajectories of the  
39 nucleation growth/ burst events were calculated using the HYSPLIT model (Hybrid Single  
40 Particle Lagrangian Integrated Trajectory, Version 4.9), in order to trace the origin of the air  
41 masses. It should be noted that the grid resolution of the meteorological data used for back-  
42 trajectories calculation was 1 x 1 degrees in latitude and longitude. The data resolution is not

1 accurate enough to trace the detailed air mass passage over the scale of this study region, and  
2 therefore, it only provides an indication from which region the air mass comes from.

3 The gaseous data available for Pinkenba included CO, NO<sub>2</sub>, and SO<sub>2</sub>, while only CO and  
4 NO<sub>2</sub> data were available for South Brisbane. The emission ratios of CO/NO<sub>2</sub> and SO<sub>2</sub>/NO<sub>2</sub>  
5 were calculated. On average, the daily minimum of each gaseous species, representing the  
6 background value, almost reached zero in our study region. Therefore we did not subtract the  
7 background data for the emission ratio calculations, as it was negligible. 48-h back  
8 trajectories were calculated for the first two sampling hours of each event (see supplementary  
9 figures S2 and S3) and the average CO/NO<sub>2</sub> and SO<sub>2</sub>/NO<sub>2</sub> concentrations measured at  
10 Pinkenba during the event period were 89.7 and 0.57, respectively. Overall, the CO/NO<sub>2</sub> ratio  
11 exceeded the ratios reported in the 2008/2009 National Pollution Inventory (from  
12 [www.npi.gov.au](http://www.npi.gov.au), accessed on 15 January 2011) for other sources, such as vehicles (9.7), oil  
13 refineries (6.4), ships (0.69) and wildfires (24.6). If the pollution plume was contributed by  
14 single source, it was possible to identify the emission source by comparing these emission  
15 ratios. For example, the ratio for SO<sub>2</sub>/NO<sub>2</sub> (0.57) was very close to the ship emission ratio of  
16 0.69. Although back-trajectory analysis found that almost all trajectories originated from the  
17 NE sector during the nucleation burst events, air masses from the NE were influenced by a  
18 number of different sources, such as ship, aircraft, oil refinery and the local vehicle emissions.  
19 Therefore, it was difficult to identify the specific source/s which contributed to the nucleation  
20 burst events. In addition, primary pollution plumes (e.g. CO and NO<sub>2</sub>) were observed at  
21 Pinkenba 1-3 hrs prior to the start of the nucleation burst events. From these results, we can  
22 conclude that the nucleation burst events were most likely influenced by industrial emissions  
23 from the area NE of the sampling site. As mentioned in section 3.4.2, the nucleation burst  
24 event could be associated to other possible sources, however the particle growth process  
25 could have been suppressed by unfavourable conditions, the exact nature of which is not  
26 known

27 For nucleation growth events, the CO/NO<sub>2</sub> ratio obtained from South Brisbane was 10.2,  
28 which is close to the emission inventory data for vehicles (9.7). Back-trajectory analysis also  
29 showed that the air masses originated from S-SW directions, except on 21/10/2009, which  
30 suggests that vehicle exhaust emissions contributed to the nucleation growth event.

31

## 32 4. Conclusion

33 A year long measurement campaign of the size distribution of ultrafine particles was  
34 conducted at subtropical urban area of Brisbane, Australia during 2009. The annual average  
35  $N_{\text{UFP}}$ ,  $N_{\text{Aitken}}$  and  $N_{\text{nuc}}$  were  $9.3 \times 10^3$ ,  $3.7 \times 10^3$  and  $5.6 \times 10^3 \text{ cm}^{-3}$ , respectively. Small  
36 seasonal variation in number concentration was observed, with higher particle concentrations  
37 observed during the warmer months. Diurnal variation of  $N_{\text{UFP}}$ ,  $N_{\text{Aitken}}$  and  $N_{\text{nuc}}$  showed the  
38 influence of local traffic exhaust emissions on the particle number concentration during  
39 morning peak hours, and elevated nucleation mode particle levels suggested the contribution  
40 of new particle formation during the early afternoon. In relation to wind direction,  $N_{\text{Aitken}}$  and  
41  $N_{\text{nuc}}$  were associated with NE winds, which pointed to the emission sources present at the

1 lower reaches of Brisbane river (such as Brisbane Airport, the oil refinery and the Port of  
2 Brisbane). A broad peak of  $N_{\text{Aitken}}$  particles was also observed during SSE to WNW winds,  
3 which suggested the influence of local traffic exhaust emissions, with particle size ranging  
4 from 30 - 70 nm. Overall, two major sources of  $N_{\text{nuc}}$  were identified in this study, which were  
5 new particle formation by nucleation and primary nucleation mode particles emitted from  
6 aircraft at Brisbane Airport. New particle formation via nucleation process was frequently  
7 observed in this study, and the particle growth rate (average  $4.6 \text{ nm hr}^{-1}$ ) was positively  
8 related to the strength of global solar radiation. The nucleation events with particle growth  
9 were associated with SW winds which suggested the influence of precursors emitted from  
10 traffic exhaust emission in Brisbane city. An interesting question arose during the course of  
11 this study regarding the absence of nucleation particle growth in air masses originating from  
12 the coast. It may due to lack of nucleation particles precursor associated with coastal air mass.  
13 To tackle this question, a further study on the new particle formation, with parallel  
14 measurements of particle chemical composition and gaseous pollutants, is needed.

15

## 16 Acknowledgements

17 This project was supported by the Australian Research Council and Queensland Transport  
18 through Linkage Grant LP0882544. We would also like to thank the Queensland Bureau of  
19 Meteorology for providing the meteorological data.

20

## 21 References

22 Charlson, R.J., Schwartz, S.E., Hales, J.M., Cess, R.D., Jr. Coakley, J.A., Hansen, J.E.,  
23 Hofmann, D.J.: Climate forcing by anthropogenic aerosols, *Science*, 255, 423-430, 1992.

24 Dal Maso, M., Kulmala, M., Riipinen, I., Wagner, R., Hussein, T., Aalto, P.P., Lehtinen,  
25 K.E.J.: Formation and growth of fresh atmospheric aerosols eight years of aerosol size  
26 distribution data from SMEAR II, Hyytiälä, Finland, *Boreal Environment Research*, 10, 323-  
27 336, 2005.

28 Donaldson, K., Li, X.Y., MacNee, W.: Ultrafine (nanometre) particle mediated lung injury,  
29 *Journal of Aerosol Science* 29, 553-560, 1998.

30 Fernández-Camacho, R., Rodríguez, S., de la Rosa, J., Sánchez de la Campa, A.M., Viana,  
31 M., Alastuey, A., Querol, X.: Ultrafine particle formation in the inland sea breeze airflow in  
32 Southwest Europe, *Atmospheric Chemistry and Physics Discussions*, 10, 17753-17788, 2010.

33 Gao, J., Wang, T., Zhou, X., Wu, W., Wang, W.: Measurement of aerosol number size  
34 distributions in the Yangtze River Delta in China: Formation and growth of particles under  
35 polluted conditions, *Atmospheric Environment*, 43, 829-836, 2009.

36 Guo, H., Ding, A., Morawska, L., He, C., Ayoko, G., Li, Y., Hung, W.: Size distribution and  
37 new particle formation in subtropical eastern Australia, *Environmental Chemistry*, 5, 382-390,  
38 2008.

39 Hussein, T., Karppinen, A., Kukkonen, J., Härkönen, J., Aalto, P.P., Hämeri, K., Kerminen,  
40 V-M., Kulmala, M.: Meteorological dependence of size-fractionated number concentrations  
41 of urban aerosol particles, *Atmospheric Environment*, 40, 1427-1440, 2006.

- 1 Hussein, T., Puustinen, A., Aalto, P.P., Mäkelä, J.M., Hämeri, K., Kulmala, M.: Urban  
2 aerosol number size distribution, *Atmospheric Chemistry and Physics*, 4, 391-411, 2004.
- 3 Johnson, G.R., Ristovski, Z.D., Anna, B.D., Morawska, L.: The hygroscopic behaviour of  
4 partially volatilized coastal marine aerosols using the VH-TDMA technique, *Journal of*  
5 *Geophysical Research*, 110, (D20203), doi:10.1029/2004JD005657, 2005.
- 6 Kim, S., Shen, S., Sioutas, C., Zhu, Y., Hinds, W.C.: Size Distribution and Diurnal and  
7 Seasonal Trends of Ultrafine Particles in Source and Receptor Sites of the Los Angeles Basin,  
8 *Air and Waste Management Association*, 52:33, 2955-2968, 2002.
- 9 Kulmala, M.: How Particles Nucleate and Grow, *Science*, 302, 1000 – 1001, 2003.
- 10 Kulmala, M., Vehkamäki, H., Petäjä, T., Dal Maso, M., Lauri, A., Kerminen, V.-M., Birmili,  
11 W., McMurry, P.H.: Formation and growth rates of ultrafine atmospheric particles: a review  
12 of observations, *Journal of Aerosol Science*, 35, 143-176, 2004.
- 13 Lee, Y., Lee, H., Kim, M., Choi, C.Y., Kim, J.: Characteristics of particle formation events in  
14 the coastal region of Korea in 2005, *Atmospheric Environment*, 42, 3729-3739, 2008.
- 15 Mazaheri, M., Johnson, G.R., Morawska, L.: Particle and Gaseous Emissions from  
16 Commercial Aircraft at Each Stage of the Landing and Takeoff Cycle, *Environmental*  
17 *Science and Technology*, 43, 441 – 446, 2009.
- 18 Mejía, J.F., Morawska, L.: An investigation of nucleation events in a coastal urban  
19 environment in the Southern Hemisphere, *Atmospheric Chemistry and Physics*, 9, 7877-7888,  
20 2009.
- 21 Mejía, J.F., Wraith, D., Mengersen, K., Morawska, L.: Trends in size classified particle  
22 number concentration in subtropical Brisbane, Australia, based on a 5 year study,  
23 *Atmospheric Environment*, 41, 1064-1079, 2007.
- 24 Meyer N.K., Ristovski, Z.: Ternary nucleation as a mechanism for the production of diesel  
25 nanoparticles: Experimental analysis of the volatile and hygroscopic properties of diesel  
26 exhaust using the volatilization and humidification tandem differential mobility analyzer,  
27 *Environmental Science and Technology*, 41, 7309-7314, 2007.
- 28 Modini, R., Ristovski, Z., Johnson, G.R., Congrong, H., Surawski, N., Morawska, L., Suni,  
29 T., Kulmala, M.: New particle formation and growth at a remote, sub-tropical coastal location,  
30 *Atmospheric Chemistry and Physics*, 9 (19), 7607-7621, 2009.
- 31 Moore, K.F., Ning, Z., Ntziachristos, L., Schauer, J.J., Sioutas, C.: Daily variation in the  
32 properties of urban ultrafine aerosol – Part I: Physical characterization and volatility,  
33 *Atmospheric Environment*, 41, 8633-8646, 2007.
- 34 Morawska, L., Thomas, S., Bofinger, N., Wainwright, D., Neale, D.: Comprehensive  
35 characterization of aerosols in a subtropical urban atmosphere: Particle size distribution and  
36 correlation with gaseous pollutants, *Atmospheric Environment*, 32, 2467-2478, 1998.
- 37 Morawaska, L., Ristovski, Z., Jayaratne, E.R., Keogh, D.U., Ling, X.: Ambient nano and  
38 ultrafine particles from motor vehicle emissions: Characteristics, ambient processing and  
39 implications on human exposure, *Atmospheric Environment*, 42, 8113-8138, 2008.

- 1 O'Dowd, C.D., McFiggans, G., Greasey, D.J., Pirjola, L., Hoell, C., Smith, M.H., Allan, B.J.,  
2 Plane, J.M.C., Heard, D.E., Lee, J.D., Pilling, M.J., Kulmala, M.: On the photochemical  
3 production of new particles in the coastal boundary layer, *Geophysical Research Letters*, 26,  
4 1707-1710, 1999.
- 5 Olivares, G., Johansson, C., Strom, J., Hasson, H.-C.: The role of ambient temperature for  
6 particle number concentrations in a street canyon, *Atmospheric Environment*, 41 (10), 2145-  
7 2155, 2007.
- 8 Park, K., Park, J.Y., Kwak, J-H., Cho, G.N., Kim, J.-S.: Seasonal and diurnal variations of  
9 ultrafine particle concentration in urban Gwangju, Korea: Observation of ultrafine particle  
10 events, *Atmospheric Environment*, 42, 788-799, 2008.
- 11 Pérez., N., Pey, J., Cusack, M., Reche, C., Querol, X., Alastuey, A., Viana, M.: Variability of  
12 Particle Number, Black Carbon, and PM10, PM2.5, and PM1 Levels and Speciation:  
13 Influence of Road Traffic Emissions on Urban Air Quality, *Aerosol Science and Technology*,  
14 44, 487 – 499, 2010.
- 15 Pey, J., Querol, X., Alastuey, A., Rodríguez, S., Putaud, J.P., Van Dingenen., R.: Source  
16 apportionment of urban fine and ultra-fine particle number concentration in a Western  
17 Mediterranean city, *Atmospheric Environment*, 43, 4407-4415, 2009.
- 18 Pey, J., Rodríguez, S., Querol, X., Alastuey, A., Moreno, T., Putaud J.P., Van Dingenen, R.:  
19 Variations of urban aerosols in the western Mediterranean, *Atmospheric Environment*, 42,  
20 9052-9062, 2008.
- 21 Ristovski, Z.D., Suni, T., Kulmala, M., Boy, M., Meyer, N.K., Duplissy, J., Turnipseed, A.,  
22 Morawska, L., Baltensperger, U.: The role of sulphates and organic vapours in growth of  
23 newly formed particles in a eucalypt forest, *Atmospheric Chemistry and Physics*, 10, 2919-  
24 2926, 2010.
- 25 Rodríguez, S., Cuevas, E., González, Y., Ramos, R., Romero, P.M., Pérez, N., Querol, X.,  
26 Alastuey, A.: Influence of sea breeze circulation and road traffic emissions on the  
27 relationship between particle number, black carbon, PM1, PM2.5 and PM2.5-10  
28 concentrations in a coastal city, *Atmospheric Environment*, 42, 6523-6534, 2008.
- 29 Qian, S., Sakurai, H., McMurry, P.H.: Characteristics of regional nucleation events in urban  
30 East St. Louis, *Atmospheric Environment*, 41, 4119-4127, 2007.
- 31 Sinha, P., Hobbs, P.V., Yokelson, R.J., Christian, T.J., Kirchstetter, T.W., Bruintjes, R.:  
32 Emissions of trace gases and particles from two ships in the southern Atlantic Ocean,  
33 *Atmospheric Environment*, 37, 2139-2148, 2003.
- 34 Suni, T., Kulmala, M., Hirsikko, A., Bergman, T., Laakso, L., Aalto, P.P., Leuning, R.,  
35 Cleugh, H., Zegelin, S., Hughes, D., van Gorsel, E., Kitchen, M., Vana, M., Hörrak, U.,  
36 Mirme, S., Mirme, A., Sevanto, S., Twining, J., Tardos, C.: Formation and characteristics of  
37 ions and charged aerosol particles in a native Australian Eucalypt forest, *Atmospheric  
38 Chemistry and Physics*, 8, 129 – 139, 2008.
- 39 Vehkamäki, H., Dal Maso, M., Hussein, T., Flanagan, R., Hyvärinen, A., Lauros, J.,  
40 Merikanto, J., Mönkkönen, P., Pihlatie, M., Salminen, K., Sogacheva, L., Thum, T.,  
41 Ruuskanen, T.M., Keronen, P., Aalto, P.P., Hari, P., Lehtinen, K.E.J., Rannik, Ü., Kulmala,

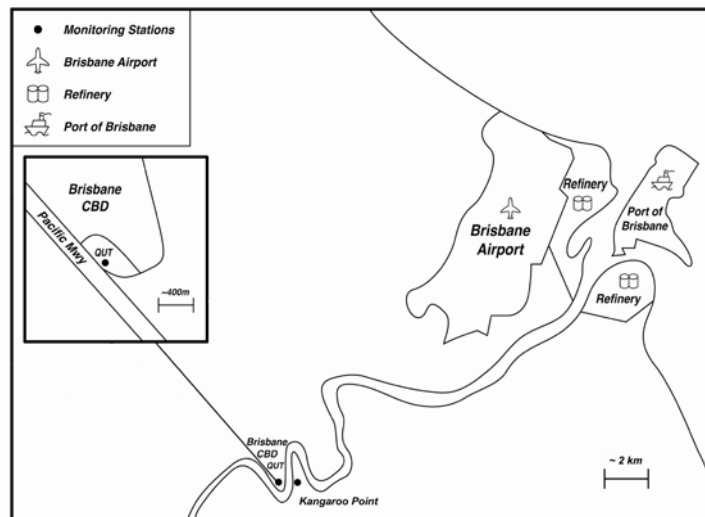
1 M.: Atmospheric particle formation events at Värriö measurement station in Finnish Lapland  
 2 1998-2002, *Atmospheric Chemistry and Physics*, 4, 2015-2023, 2004.

3 Weber, R.J., Moore, K., Kapustin, V., Clarke, A., Mauldin, R.L., Kosciuch, E., Cantrell, C.,  
 4 Eisele, F., Anderson, B., Thornhill, L.: Nucleation in the equatorial pacific during PEM-  
 5 tropics B: Enhanced boundary layer H<sub>2</sub>SO<sub>4</sub> but no particle production: NASA global  
 6 tropospheric experiment Pacific Exploratory Mission in the tropics phase B, Part 1:  
 7 Measurement and analyses (PEM-Tropics B), *Journal of Geophysical Research*, 106, 32767 –  
 8 32776, 2001.

9 Woo, K.S., Chen, D.R., Pui, D.Y.H., McMurry, P.H.: Measurements of Atlanta aerosol size  
 10 distributions: observations of ultrafine particle events, *Aerosol Science and Technology*, 34,  
 11 75-87, 2001.

12 Wu, Z., Hu, M., Lin, P., Liu, S., Wehner, B., Wiedensohler, A.: Particle number size  
 13 distribution in the urban atmosphere of Beijing, China, *Atmospheric Environment*, 42,  
 14 7967,7980, 2008.

15

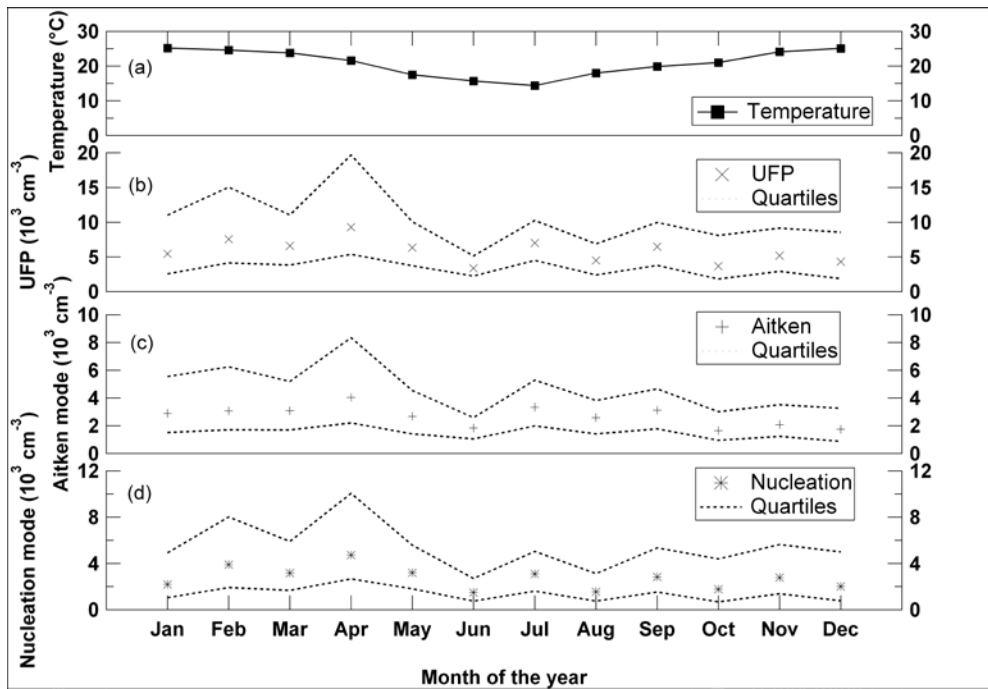


16

17

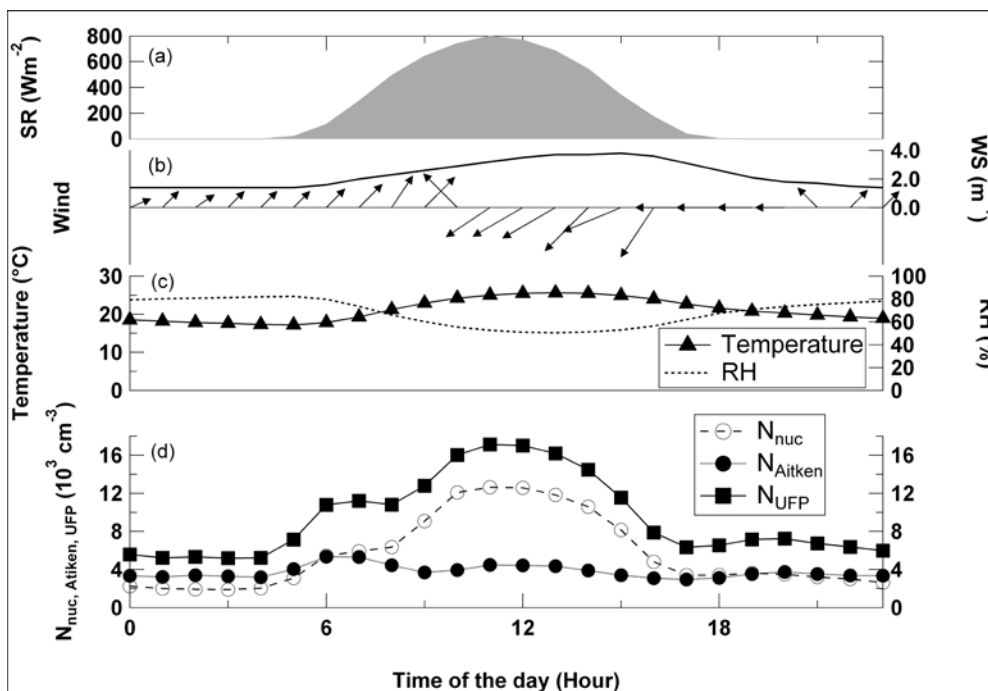
18

**Figure 1:** Map of Brisbane.



1

2 **Figure 2:** Monthly variations of (a) mean temperature, and particle number concentration of  
 3 ultrafine (UFP) (b), Aitken mode (c) and nucleation modes particles (d). The  
 4 median number concentrations and the 1<sup>st</sup> and 3<sup>rd</sup> quartiles are presented.

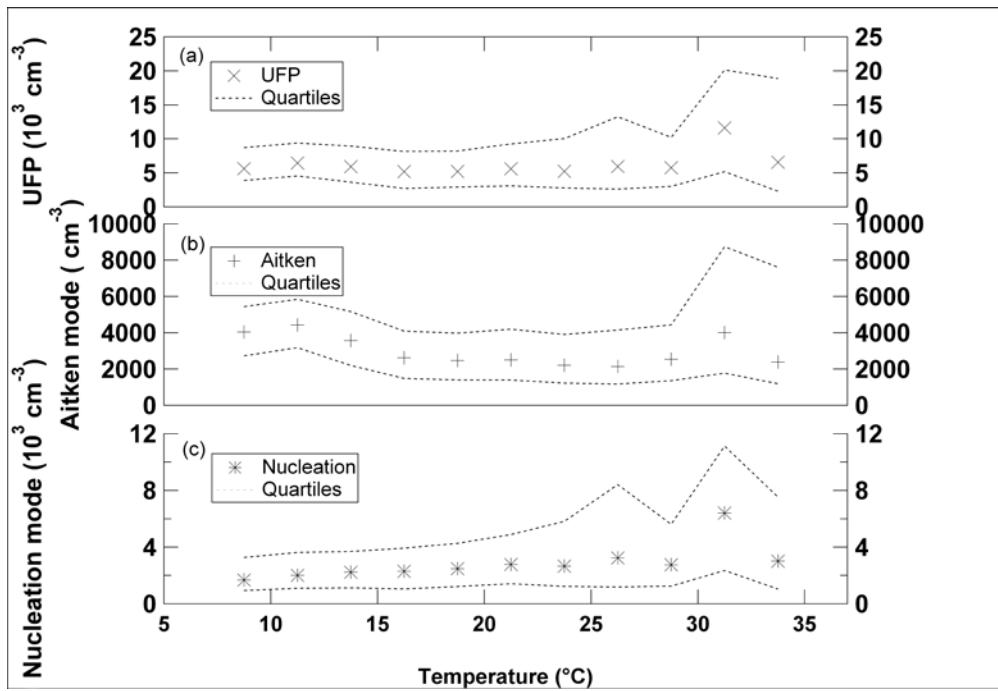


5

6 **Figure 3:** Diurnal variation of (a) averaged solar radiaiton, (b) averaged wind  
 7 direction/speed, (c) averaged temperature and RH, and (d) averaged UFP,  
 8 nucleation mode and Aitken mode particle concentrations.

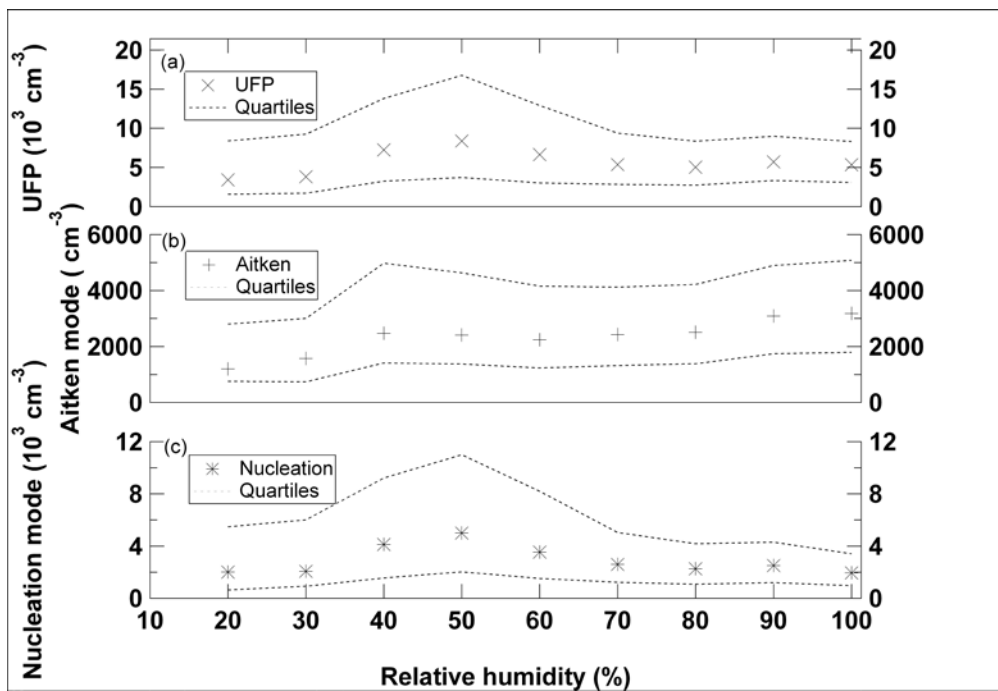
9





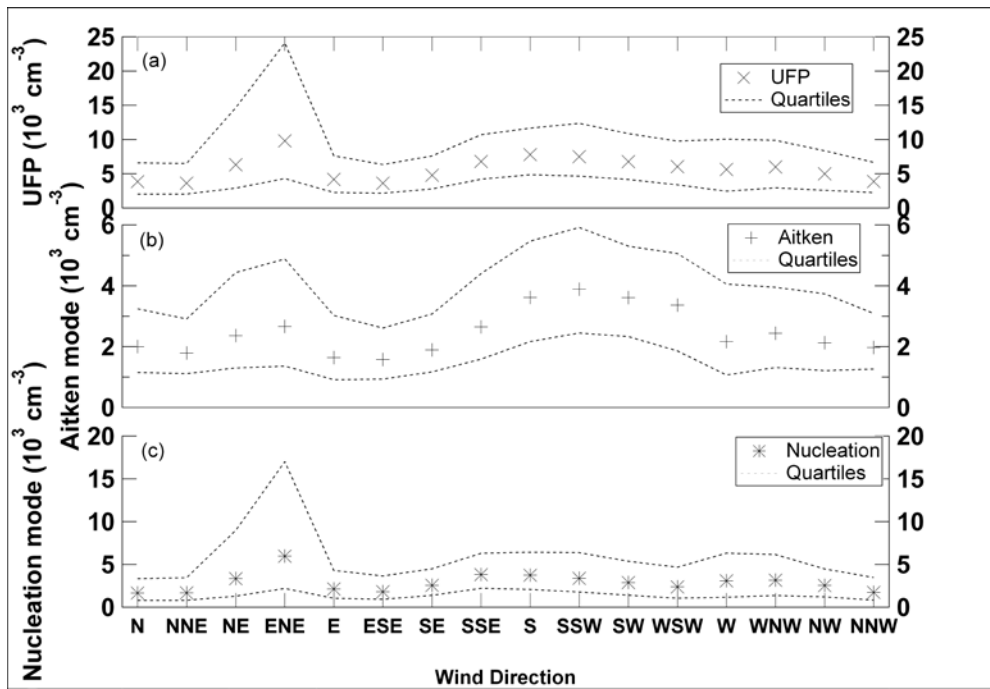
1  
2  
3  
4  
5

**Figure 4:** Particle number concentrations of (a) ultrafine (UFP), (b) Aitken mode and (c) nucleation mode particles and their variation as a function of temperature. The median number concentrations and the 1<sup>st</sup> and 3<sup>rd</sup> quartiles are presented.



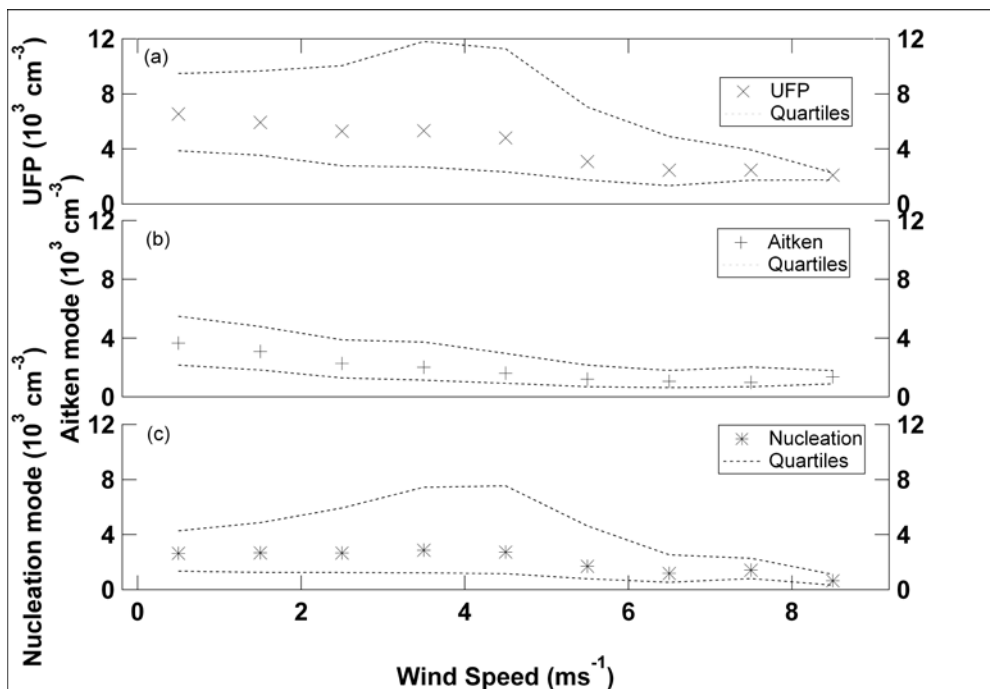
6  
7  
8  
9  
10

**Figure 5:** Number concentrations of (a) ultrafine (UFP), (b) Aitken mode and (c) nucleation mode particles and their variation as a function of relative humidity. The median number concentrations and the 1<sup>st</sup> and 3<sup>rd</sup> quartiles are presented.



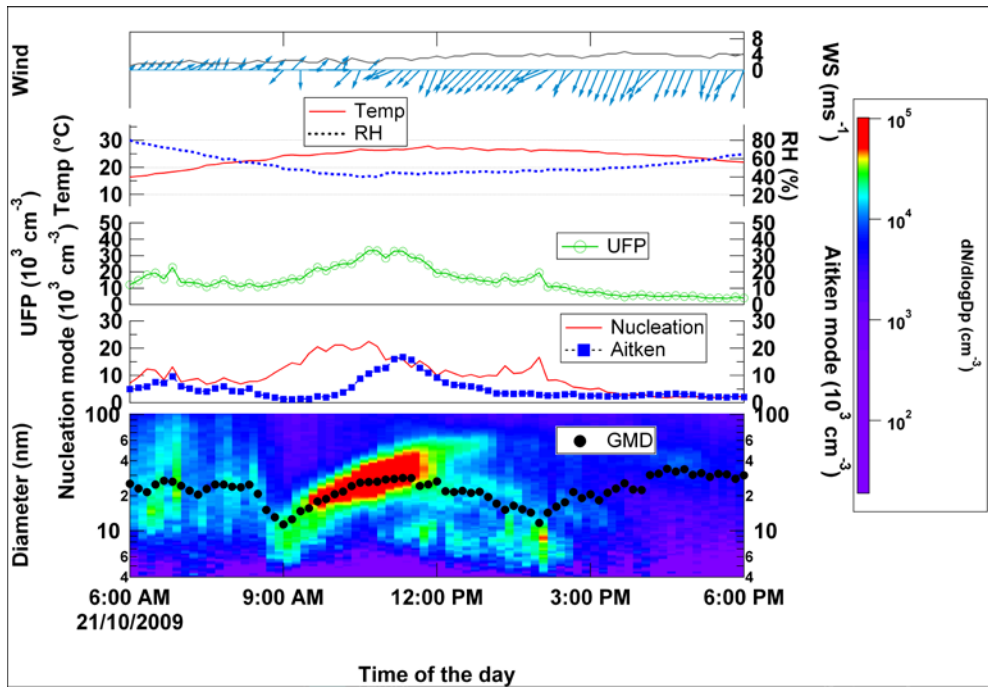
1  
2  
3  
4  
5

**Figure 6:** Number concentration of (a) ultrafine (UFP), (b) Aitken mode and (c) nucleation mode particles and their variation as a function of wind direction. The median number concentrations and the 1<sup>st</sup> and 3<sup>rd</sup> quartiles are presented.



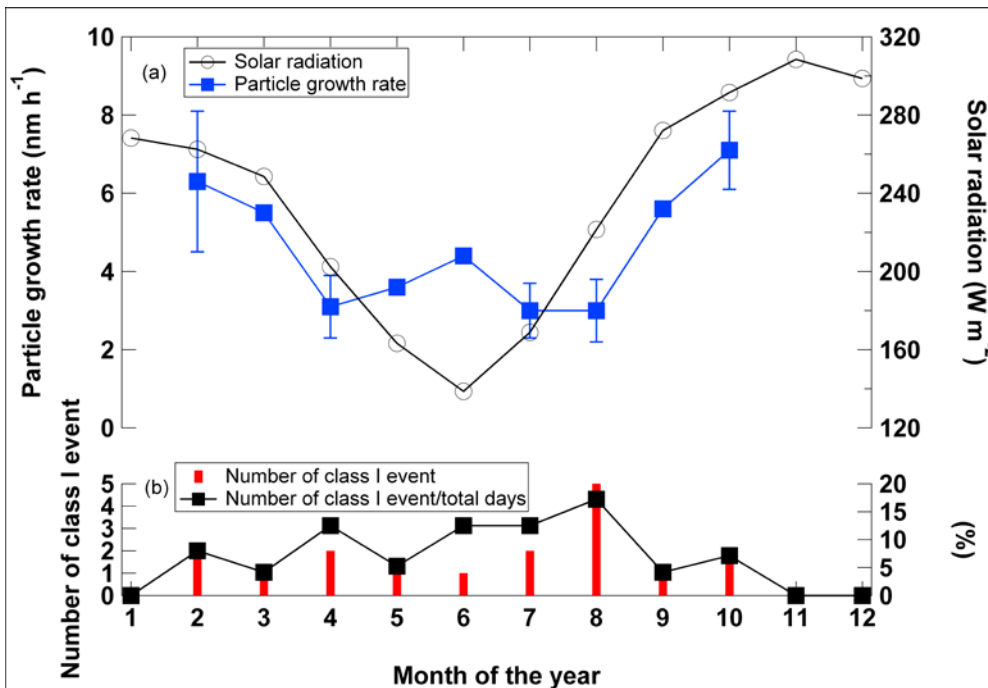
6  
7  
8  
9  
10

**Figure 7:** Number concentration of (a) ultrafine (UFP), (b) Aitken mode and (c) nucleation mode particles and their variation as a function of wind speed. The median number concentrations and the 1<sup>st</sup> and 3<sup>rd</sup> quartiles are presented.



1  
2  
3  
4  
5  
6  
7

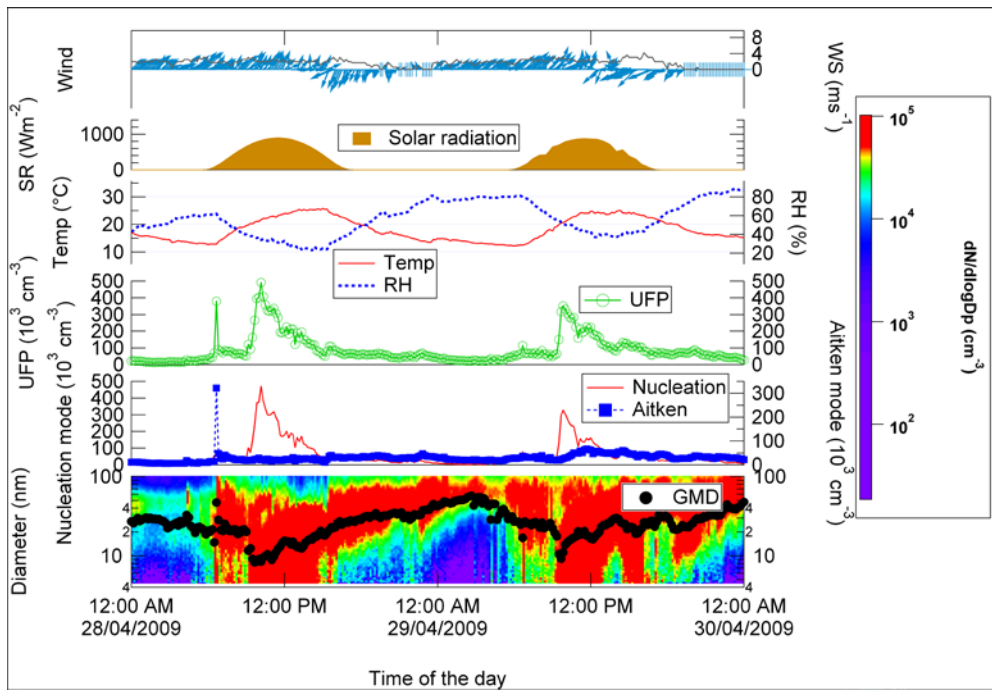
**Figure 8:** The time series of nucleation events observed at QUT on 21 October 2009. From bottom to top, the parameters are: i) Geometric median diameter (GMD) and contour plot of size distribution; ii) Particle number concentration of nucleation and Aitken mode particles; iii) Particle number concentration of ultrafine particles (UFP); iv) Temperature and relative humidity; and v) wind direction and speed.



8  
9  
10

**Figure 9:** Seasonal variation in (a) particle growth rates and solar radiation and (b) number of class I event and the percentage ratio of class I event to total sampling days.

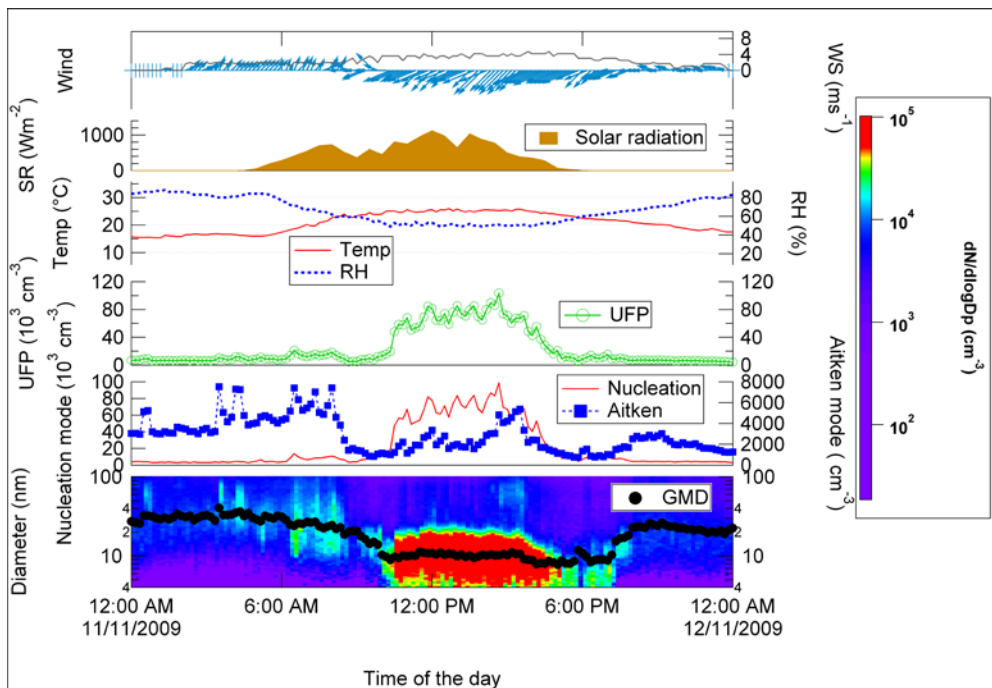
1



2

3 **Figure 10:** The nucleation events observed on 28-29 April 2009. From bottom to top, the  
 4 parameters are: i) Geometric median diameter (GMD); ii) Particle number  
 5 concentration of nucleation and Aitken mode particles; iii) Particle number  
 6 concentration of ultrafine particles (UFP); iv) Temperature and relative humidity;  
 7 v) Solar radiation; and vi) wind direction and speed.

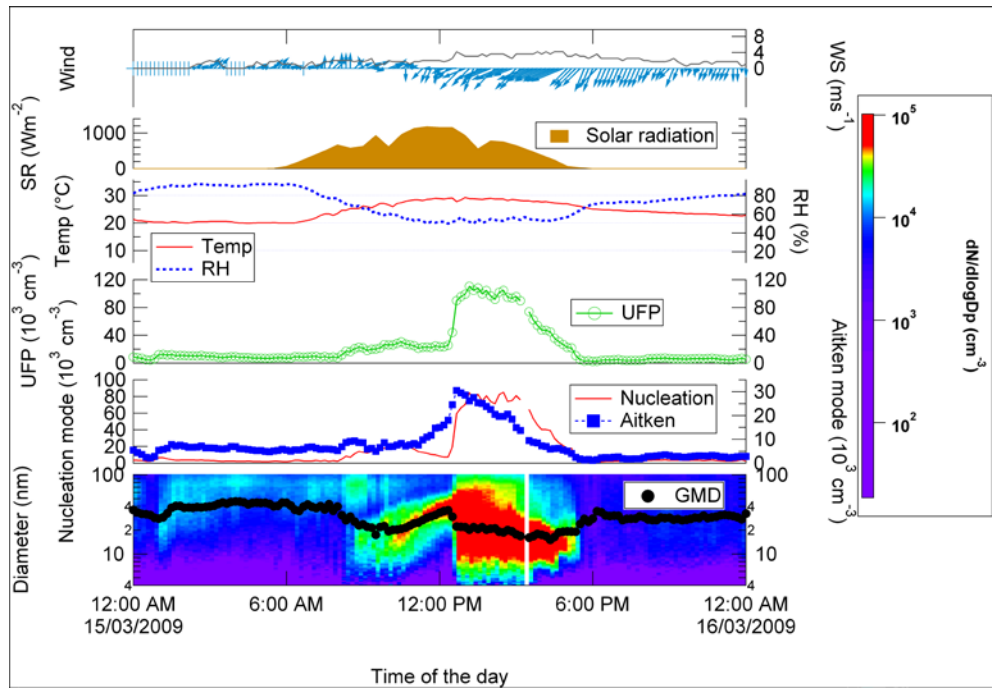
8



9

1 **Figure 11:** The nucleation bursts measured on 11 November 2009. From bottom to top, the  
 2 parameters are: i) Geometric median diameter (GMD); ii) Particle number  
 3 concentration of nucleation and Aitken mode particles; iii) Particle number  
 4 concentration of ultrafine particles (UFP); iv) Temperature and relative humidity;  
 5 v) Solar radiation; and vi) wind direction and speed.

6



7

8 **Figure 12:** Contour plot of particle size distribution observed on 15 March 2009. From  
 9 bottom to top, the parameters are: i) Geometric median diameter (GMD) and  
 10 contour plot of size distribution; ii) Particle number concentration of nucleation  
 11 and Aitken mode particles; iii) Particle number concentration of ultrafine particles  
 12 (UFP); iv) Temperature and relative humidity; v) Solar radiation; and vi) wind  
 13 direction and speed.

14

15

16

17

18

19

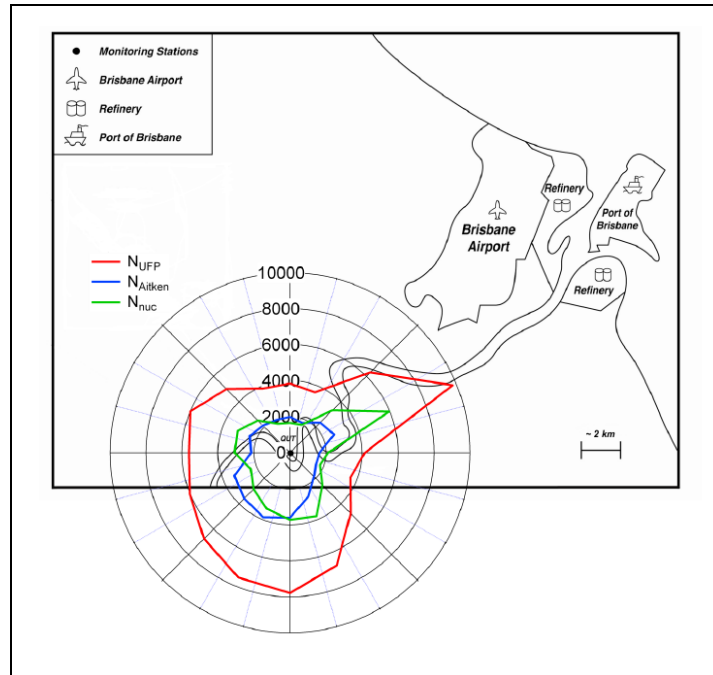
20

21

22

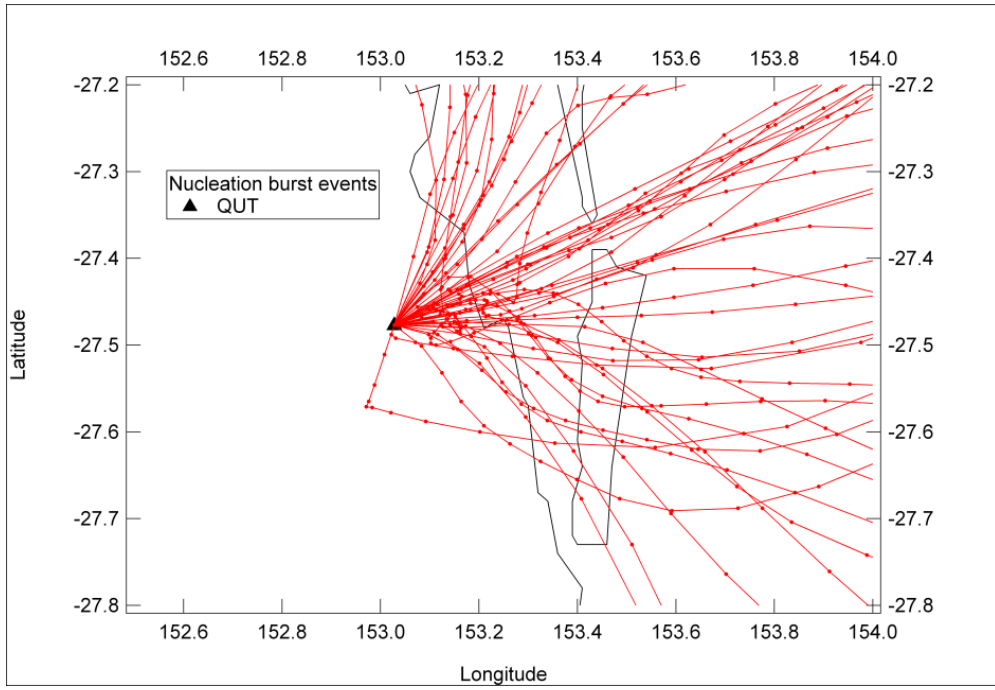
1  
2  
3  
4  
5  
6

## Supplementary materials



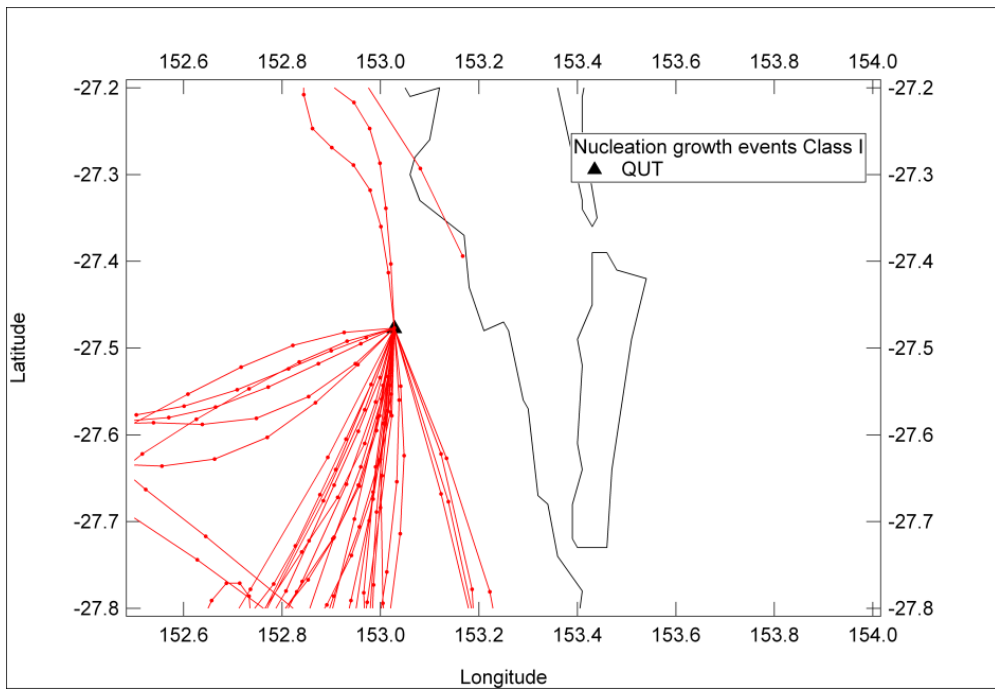
7  
8  
9  
10  
11

Figure S1: Wind rose plot of  $N_{UFP}$ ,  $N_{Aitken}$  and  $N_{nuc}$  superimposed over the location map. The origin of the wind rose is located at QUT.  $N_{UFP}$  - red line;  $N_{Aitken}$  - blue line;  $N_{nuc}$  - green line. Unit in  $\text{cm}^{-3}$ .



1  
2  
3

Figure S2. Back-trajectories calculated during the nucleation burst events.



4  
5

Figure S3. Back-trajectories calculated during the class I nucleation growth events